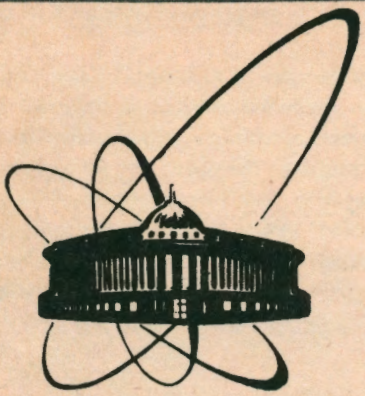

объединенный
институт
ядерных
исследований
дубна

E4-92-113

F.A.Gareev, S.N.Ershov, O.I.Melnikova, G.S.Kazacha,
E.F.Svinareva, J.S.Vaagen*

DATA-TO-DATA RELATIONS BETWEEN ELASTIC AND INELASTIC SCATTERING IN NUCLEAR RAINBOW REGION OF ANGLES

Submitted to "Physical Review"

*Institute of Physics, University at Bergen, Bergen, Norway

1992

1 Introduction

The distorted wave methods (we use this terminology for different versions of the distorted wave Born approximation, coupled channel methods, etc.) have been very useful for the description and interpretation of elastic, inelastic and direct reaction experimental data at low projectile energies. The elastic scattering data in such methods play in some sense an auxiliary role to establish the parameters of the optical potential. Further the distorted waves, calculated with the best fitted optical model parameters, are incorporated for the calculations of the corresponding amplitudes for different processes. Therefore the interplay between the elastic scattering and different direct processes in such calculations is hidden. It is well known that the reactions depend not only on the nucleus-nucleus potential which determines the relative motions, but also on the reaction form factors. This means that the structure of amplitudes for elastic scattering and inelastic scattering are nonidentical.

With increasing the projectile energies the theoretical treatment of strongly coupled collective states can be simplified because the energy of the collective states is small as compared with the incident projectile energy. This gives strong arguments for applying the adiabatic approximation at intermediate energies. Drozdov [1] and Inopin [2] introduced the adiabatic approximation for the inelastic Fraunhofer diffractive scattering from strongly absorbing nuclei within a sharp radius R_0 with the quadrupole surface deformation or quadrupole surface vibration. Further Blair [3] extended this method for deformations of arbitrary multipolarity and obtained his well-known phase rule exploiting the asymptotic properties of Bessel functions. The Blair phase rule was exploited very successfully to establish the parity and the angular momentum for collective states from the experimental cross sections. At $R_0\theta k \gg 1$ one can get the relations between the cross sections of the elastic and inelastic scattering data (further data-to-data relations in accordance with terminology from [4]).

Data-to-data relations have been derived for proton-nucleus scattering in [4] at intermediate energies and for large momenta transfer starting with an eikonal expression for the amplitude and exploiting the asymptotic properties of the corresponding integral and the nuclear property via the method of stationary phase neglecting the Coulomb interactions.

Data-to-data relations have been established [5] for the isovector giant dipole resonances and isoscalar giant quadrupole resonances in the Coulomb rainbow region of the angles and a very good agreement with data is obtained.

In this article we will investigate the question of validity of the data-to-data relation between elastic and inelastic scattering cross sections in the Fraunhofer diffractive region of angles and for greater angles in the presence of nuclear "rainbow-like" phenomena. Our aim is to investigate the problem: how the presence of the form factors in inelastic amplitude modifies the corresponding cross sections and does the presence of the pronounced nuclear "rainbow-like" effects in the elastic scattering ensure that the same effects will be observed in the inelastic scattering.

2 General relations

i)Here we have summarized the results obtained by Amado et al. [4] using a distorted wave impulse approximation with the eikonal treatment of the distortion and stationary phase method exploiting the asymptotic form of the Bessel function. Thus the inelastic scattering cross section in terms of the elastic scattering one is given by

$$\sigma_{in,L}(q) = \mid \frac{\lambda_L}{\gamma} \mid^2 \frac{2L+1}{4\pi} \mid b_{st} \mid^{2(L-2)} exp(2\pi a\Phi/R)(\mid b_{st} \mid q)^2 \sigma_{el}(Rq+\Phi), \quad (1)$$

where b_{st} is the impact parameter at the stationary point given by

$$b_{st} = \mid b_{st} \mid e^{i\phi} = R + i\pi a, \quad (2)$$

with R the nuclear radius and the skin thickness parameter appropriate to a Fermi distribution

$$\rho(r) = \rho_0[1 + exp(\frac{r-R}{a})]^{-1}, \quad (3)$$

where $\Phi = (L-1)\phi + \eta$ and $\eta = 0$ for odd L and $\pi/2$ for even L. This is the general result of [4] as we will show below. It relates the inelastic cross section for excitation of a collective state of spin L at angle θ to the cross section for elastic scattering at the angle $\theta + \Phi/kR$ in terms of purely kinematic factors and the overall strength of the excitation $\mid \lambda_L \mid^2$, determined in the Tassie model [6]. In ref.[4] it has been shown that in the cases of $^{208}Pb(p,p')$ and $^{54}Fe(p,p')$ at E_p=800 MeV data-to-data asymptotic formulas (1) reproduce the data shape and general magnitude except at small angles where the Coulomb interaction is dominated and the asymptotic approximation fails.

ii)In the framework of the Drosdov-Inopin-Blair model [1, 2, 3] the inelastic scattering cross section, under the condition $R_0 k\theta = R_0 q \gg 1$ (R_0 is a strongly absorbing sharp radius), can be rewritten in terms of the elastic scattering cross section:

$$\sigma_{in,L}(\theta) = \frac{2L+1}{8\pi} \frac{\hbar\omega_L}{C_L} (R_0 q)^2 \sigma_{el}(R_0 q + \phi_L), \quad (4)$$

where $\phi_L = \pi/4$ for even L and $\phi_L = -\pi/4$ for odd L.

iii)If we consider the elastic and inelastic diffractive scattering from the potential V(r)

$$V(r) = V_0, \qquad r < R = R_0(1 + \sum_{LM} \alpha_{LM} Y_{LM});$$
$$V(r) = 0, \qquad r > R, \quad (5)$$

in the Born approximation with plane-wave initial and final wave functions, then we can re-express the results of ref.[7] in the following way

$$\sigma_{in,L}(\theta) = \frac{1}{4\pi} \sum_{M'M} \mid < L'M' \mid \alpha_{LM} \mid 00 >^2 (R_0 q)^2 \sigma_{el}(R_0 q + \phi_L). \quad (6)$$

We would like to stress that expressions (1), (4) and (6) are quite similar. They are obtained for the strongly absorbing case except (1) where a more flexible model is used.

All formulas show clearly the geometric origin of the elastic and inelastic scattering. We see the connection between cross sections of elastic and inelastic scattering and can understand why the use of optical potentials which accurately fit the elastic scattering is expected to give good fits to inelastic angular distributions. An accurate fit of elastic scattering gives accurate distorted wave functions, both in the outer region of the nuclear surface and at larger radii, and in these regions the wave function is fully determined by the η_L ($S_L = \eta_L exp(i2\delta_L)$) parameters of elastic scattering, rather than by details of the optical potential. It is generally assumed that the Fraunhofer diffractive elastic scattering is not sensitive to the detailed shape of the absorption potential W(r) for distances smaller than the radius of strong absorption R_{abs}, and that W(r) here is more or less arbitrary, as long as it gives the necessary absorption. Moreover, the period of the Fraunhofer diffractive oscillations is determined by the radius of strong absorption: $\Delta\theta = \pi/kR_{abs}$. It is possible to introduce the corrections [8, 9] due to the Coulomb interaction and the diffuse edges of the nuclei, the latter correction leads to the additional factorized damping factor into the expression for the amplitude and makes the cross section fall more rapidly as the angle θ increases.

In the derivation of formulas (1), (4) and (6) we used $q \mid b_{st} \mid$ and qR_0 large. Therefore they might be expected not to work for forward angles.

Amado et. al. [4] show that the asymptotic formula (1) gives an excellent description of the data shape and general magnitude (for the excitation of the 2.6 MeV 3^- and 3.2 MeV 5^- states in ^{208}Pb by 800 MeV protons) except in the forward direction as expected. The authors write that "we have also seen that data-to-data formulas do even better job of fitting the details of the data and remove some inadequacies in the simple asymptotic data." We believe that this conclusion is true for a wider class of processes, where strong absorption and refraction will concentrate the excitation mechanism on the surface. It means that it is very interesting to use the data-to-data formulas for different probes in a wide region of projectile energies.

3 Surface reactions

In this section we will follow a Glauber-like (eikonal approximation for the distorted waves) approximation to analyse the excited states in heavy-ion collisions at intermediate energies [10]. In this approximation the amplitude for transition from the ground state $\mid 0 >$ to the excited state $\mid LM >$ is given by

$$f^{LM}_{N,C}(\theta) = \frac{ik}{2\pi\hbar v} \int e^{i(\vec{q}\cdot\vec{r}) - \chi(b)} < \vec{r}, LM \mid U_{N,C}(\vec{r}) \mid \vec{r}, 00 > d\vec{r}, \quad (7)$$

where

$$\chi(b) = i\frac{k}{E} \int_0^\infty [U_C(\sqrt{b^2+z^2}) + U_N(\sqrt{b^2+z^2})] dz. \quad (8)$$

The authors of ref.[10] used the $t\rho\rho$ approximation for the nuclear interaction and parametrized the nuclear densities by Gaussians

$$\rho^{(i)}(r) = \rho^i_O e^{-r^2/\alpha_i^2}, \quad (9)$$

which are sufficiently good for our purpose. We can now rewrite the result of [10] slightly modifying the notation (using $(\vec{q}\bullet\vec{r}) \approx (\vec{q}\bullet\vec{b}) = qbcos\phi$):

$$f_N(\theta) = ikB_L \int_0^\infty dbbJ_M(qb)e^{-\chi(b)} \int_{-\infty}^\infty dzr^L \frac{1}{r}\frac{d}{dr}\rho(r)P_{LM}(\theta)i^{-M}, \qquad (10)$$

where B_L is the excitation strength and ρ is the effective nuclear density obtained in the folding procedure

$$\rho(r) = 2\pi^{3/2}\frac{\alpha_1^3\alpha_2^3}{\alpha^3}\rho_G^{(1)}\rho_G^{(2)}e^{-r^2/\alpha^2}, \qquad (11)$$

$$\alpha^2 = \alpha_1^2 + \alpha_2^2, \qquad (12)$$

$$\chi(b) = \gamma t(b) = \gamma\int_{-\infty}^\infty \rho(\sqrt{b^2+z^2})dz. \qquad (13)$$

We may conclude that the transition amplitude (10) has the same form as in ref. [4] except that we used the Gaussians (9) for the nuclear densities while the authors in [4] used the Fermi distribution (3). Therefore all conclusions of [4] are also correct for data-to-data relations in our case provided that $R \rightarrow Reb_{st}$ and $\pi a \rightarrow Imb_{st}$. For the case of a 1^- state we obtain an extremely simple result exactly as in [4]:

$$\sigma_{in,1^-}(q) = \mid \frac{\lambda_1}{\gamma} \mid^2 \frac{3}{4\pi}q^2\sigma_{el}(q), \qquad (14)$$

We do not expect the eikonal approximation to be correct for the description of the nuclear rainbow scattering where the conditions of applicability of this approximation do not fulfill. Nevertheless we can use the eikonal approximation for qualitative estimations to establish the data-to-data relations in the nuclear rainbow region at the angles where the far-side amplitude is dominated over the near-side one. It is easy to get formulas similar to (1).

It is very interesting to stress that the data-to-data relations for the excitations of isovector giant dipole and isoscalar giant quadrupole resonances have been established in the Coulomb rainbow region of angles.

Therefore we can expect that for a wide class of surface reactions, if the transition densities can be approximated by the Tassie-like form, the data-to-data relations will fulfill in a wide region of angles except the angles involving the strong Coulomb-nuclear interferences. We will below restrict ourselves to the consideration of the cases when nuclear rainbow-like phenomena are present in the elastic and inelastic scattering.

4 Test of data-to-data relations from experimental data

In Fig.1 the cross sections of elastic and inelastic scattering $^{12}C + ^{12}C$ at different projectile energies (the experimental data are taken at E=240 MeV from [11] and at E=360, 1016 and 1449 MeV from [12]) are shown. The angular distributions of the

elastic and inelastic scattering have similar features: a diffraction structure at small angles, followed by an exponential fall-off with increasing slopes when the projectile energy increase. It is interesting to note that these slopes are different for elastic and inelastic scattering: the exponential fall-off is faster for the elastic scattering than for the inelastic one. In the diffraction region the data satisfy the well known Blair phase rule. In our recent analysis of elastic and inelastic scattering of ^3He on ^{12}C at E/A$\sim$ 25 MeV/A [13, 14] we have shown that the behaviour of the cross section at angles beyond the diffraction oscillations corresponds to rainbow scattering (this question will be discussed below).

The data were analyzed by DWBA and the best fit parameters to the elastic scattering are given in table 1. The analysis has been carried out by using a six-parameter Wood-Saxon potential including volume real and imaginary parts. The inelastic form factors for the 2^+ state were chosen proportional to derivatives of the optical potential, the coefficient of the proportionality being equal to the deformation parameter β_{2+} taken as a free parameter (see table 1). The calculations reproduce both elastic and elastic scattering very well.

Table 1. Parameters for Woods-Saxon type optical potentials used for describing the elastic and inelastic scattering data $^{12}C + ^{12}C$.

E(MeV)	-V	r_V^*	a_V	-W	r_W	a_W	$\frac{J_V}{A_P A_T}$	$\frac{J_W}{A_P A_T}$
240	260	1.012	1.016	29.00	2.060	0.753	272	111
360	170	1.333	0.836	29.57	2.058	0.663	245	108
1016	130	1.368	0.889	49.34	1.767	0.692	208	122
1449	100	1.221	1.171	59.99	1.757	0.639	176	142

E(MeV)	$\frac{\chi^2}{N}(0^+)/\frac{\chi^2}{N}(2^+)$	β_2	α_2	δq
240	4.2/13.0	0.4	0.3	0.307
360	3.0/2.9	0.4	0.3	0.327
1016	1.3/3.7	0.4	0.5	0.381
1449	3.7/7.8	0.45	1.25	0.455

*) $R_i = r_i A_T^{1/3}, r_C = 1.9$

Let us return to the data-to-data relations and rewrite formula (1) in the simple notation

$$\sigma_{in,L}(q) = \alpha_L q^2 \sigma_{el}(q + \delta q), \qquad (15)$$

in which the quantities α_L and δq will be extracted from comparison of the experimental data for elastic and inelastic scattering (see table 1). The results of these manipulations are shown in Fig.2 where the full lines correspond to the genuine inelastic scattering data with excitation of the 2^+ state; and the bullets, to the calculated ones from (15) by using the elastic scattering experimental data (the elastic cross sections were multiplied by a normalization factor α_2 and shifted to δq, see table 1). One can see that the genuine inelastic cross sections and calculated ones from (15) (we will further call the calculated elastic cross sections according to (15) as modified ones) coincide very well with each other.

Therefore the above-mentioned facts tell us that the form factors of the 2^+ state in ^{12}C have the surface character and are equal to derivatives of the optical potential.

This means that the mechanism of excitation of the 2^+ state is the same as for elastic scattering, the presence of form factors in the amplitude of inelastic scattering brings an additional factor q multiplied by the strength of 2^+ excitation.

The decomposition of the elastic and inelastic cross sections into the near- and far-side cross sections is shown in Figs.3-4. The solid curves correspond to the inelastic scattering cross sections, the short dashed curves in Figs.3a, 3c, 4a, 4c, to the elastic scattering cross sections multiplied by the normalization coefficient α_2; and the long dashed ones in Figs.3b, 3d, 4b, 4d, to elastic scattering cross sections shifted to δq, multiplied by $\alpha_2 q^2$. One can see that the near- and far-side cross sections for elastic and inelastic scattering are very different while the corresponding decomposed cross sections for the inelastic and modified ones are very close except at small angles. These differences at small angles are due to the Coulomb+nuclear interference effects.

The results of the same calculations are shown in Figs.5-6 for the case $^6Li+^{12}C$ at E=210 [15] and 318 MeV [16]. The parameters of optical potentials were taken from [15, 16] (see table 2). One can see that we can make the same conclusions as for the case $^{12}C+^{12}C$.

Table 2. Parameters for Woods-Saxon type optical potentials used for describing the elastic and inelastic scattering data $^6Li+^{12}C$.

E(MeV)	-V	r_V^*	a_V	-W	r_W	a_W	$\frac{J_V}{A_P A_T}$	$\frac{J_W}{A_P A_T}$
210	113.5	1.305	0.793	34.2	1.682	0.784	298	160
318	122.5	1.144	0.902	27.6	1.706	0.914	280	148

E(MeV)	$\frac{\chi^2}{N}(0^+)$	β_2	α_2	δq
210	3.9	0.34	0.2	0.45
318	2.7	0.5	0.4	0.45

*) $R_i = r_i A_T^{1/3}, r_C = 1.9$

The results for the case $^3He+^{12}C$ at E=72 MeV are pictured in Fig.7. The parameters of the optical potential were taken from [17] (see table 3). This case is extreme in the sense that data-to-data relations are hardly applicable (λ=2.4 fm), nevertheless, the data-to-data formula gives reasonable correspondence between elastic and inelastic scattering at the rainbow angles. It is desirable to study collisions of this system at higher energies.

Table 3. Parameters for Woods-Saxon type optical potentials used for describing the elastic and inelastic scattering data $^3He+^{12}C$ at E=72 MeV.

E (MeV)	-V	r_V*)	a_V	-W	r_W	a_W	W_D	r_D	a_D
72	112.8	1.103	0.831	4.58	2.17	0.98	9.9	1.268	0.55

V_{SO}	r_{SO}	a_{SO}	$\frac{J_V}{A_P A_T}$	$\frac{J_W}{A_P A_T}$	$\frac{\chi^2}{N}(0^+)/\frac{\chi^2}{N}(2^+)$	β_2	α_2	δq
0.39	1.264	0.107	437	161	6.4/6.3	0.56	0.3	0.391

*) $R_i = r_i A_T^{1/3}, r_C = 1.25$

We hope that the data-to-data relations between elastic and the direct reactions a surface nature will be held too. In Fig.8 the results of calculations by using the data-to-data formula for the experimental data of charge-exchange reactions $^{14}C(^3He,t)^{14}N$ $(0^+, 2.31 MeV)$, $^{14}C(^3He,t)^{14}N(1^+, 3.95 MeV)$ and elastic scattering are shown (α=0.012 and δq=0.493). The correspondence between the elastic cross section and charge-exchange ones is again reasonable at the rainbow angles (the similarity between the elastic scattering and charge-exchange reactions was considered in [13]). If this correspondence is not accidental, then it gives good chances to extract the information about the form factors of charge-exchange reactions at intermediate energies.

5 Conclusion

Elastic scattering of ^3He, ^6Li and ^{12}C on ^{12}C and corresponding inelastic scattering of these systems with excitation of a low-lying 2^+ state of ^{12}C have been studied in a wide region of angles and energies. Our results seem to provide the following information.

We demonstrate that the strong absorption and refraction will concentrate the excitation mechanism of 2^+ on the surface, and due to this surface nature of the excitation, these phenomena should be geometric in nature, therefore it gives arguments for establishing the data-to-data relations between elastic and inelastic scattering cross sections containing the inelastic coupling strengths, some geometrical factors. The presence of form factors in the inelastic amplitude brings an additional factor for the inelastic cross section which is equal to $q^2 = (2k\sin(1/2\theta))^2$. This explains why the slopes of exponential fall-off for $q > 1$ are smaller for the inelastic cross sections than for the elastic ones.

Impressive success of the data-to-data relations for $q > 1$ in the description of inelastic scattering confirms the well-known sensitivity of inelastic scattering to the surface and tail of the form factor. This gives additional criteria to establish the presence of rainbow phenomena in the surface-dominated inelastic scattering. If the rainbow criteria are fulfilled for elastic scattering (see [17] for a detailed description of these criteria), then the rainbow-like phenomenon has to be observed for inelastic scattering with the excitation of collective states. We suspect that this conclusion will be true for direct surface reactions too. At least, one example of charge-exchange reactions seems to support this expectation. We come to the conclusion that the inelastic scattering and direct surface reactions data at intermediate energies will give further evidences for discriminating some ambiguities of optical potentials and the corresponding form factors.

The data-to-data relations were obtained within the eikonal approximation while the analysis was carried out at sufficiently low energies ($E/A \geq$20 MeV/A) by using the DWBA approximation and existing experimental data. It seems that either the eikonal approximation has a wider range of applicability, or the data-to-data relations could be obtained from more general approximations for the surface-nature direct reactions. The impressive success of the data-to-data relations clearly shows the usefulness of this type of relations. Further application to other systems is in progress.

The authors are grateful to profs. M. Buenerd and H. Bohlen for providing experimental data.

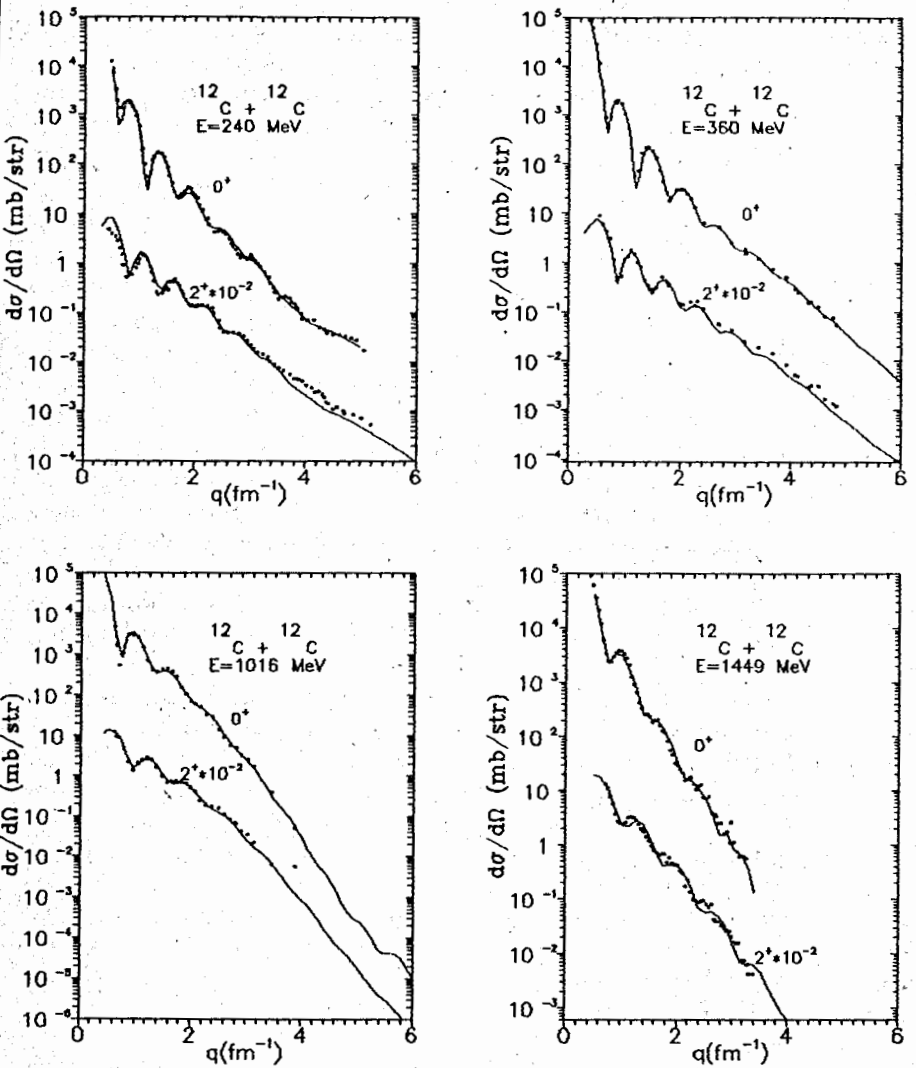

Fig.1 Experimental elastic and inelastic cross sections $^{12}C + ^{12}C$ at different energies. DWBA elastic and inelastic angular distributions for the optical potentials from table 1 are shown by solid lines.

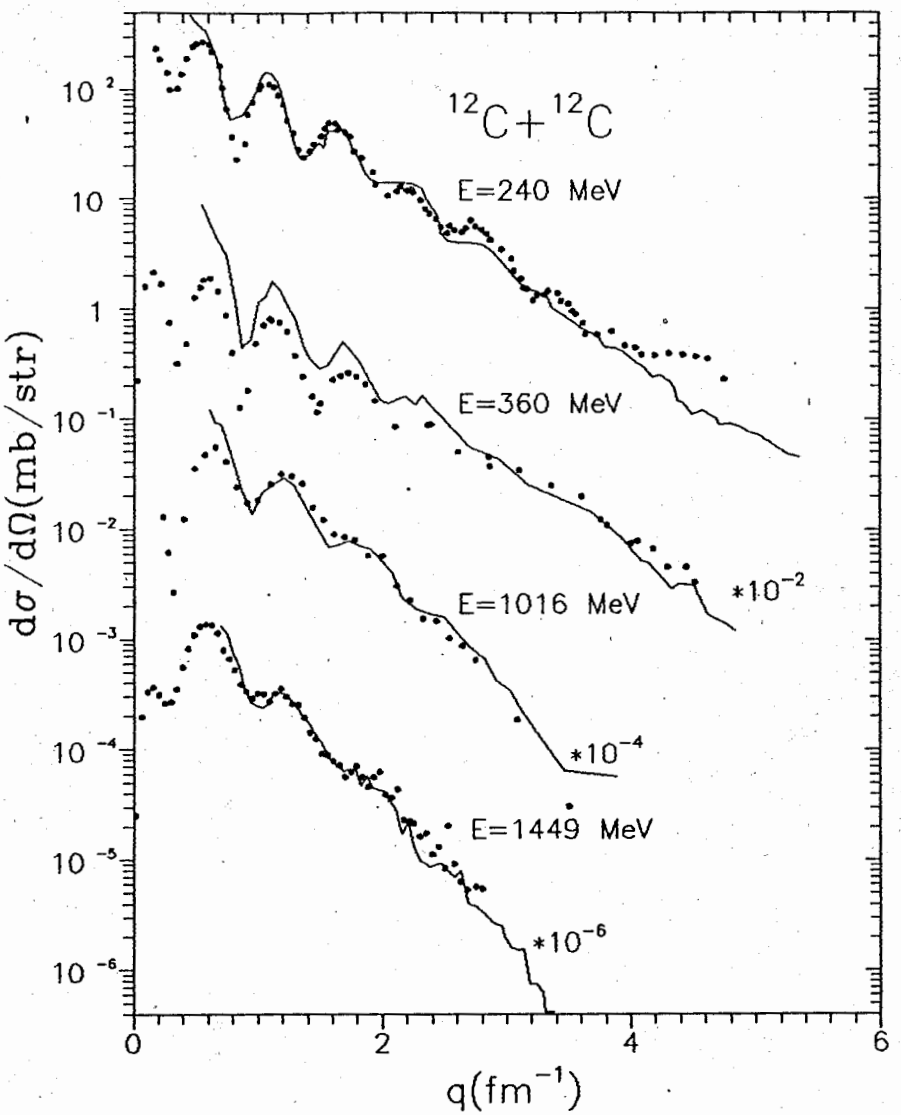

Fig.2 The correspondence between the elastic and inelastic cross sections. The full lines correspond to the genuine inelastic scattering data with excitation of the 2^+ state; and bullets, to the calculated ones from (15) by using the elastic scattering experimental data (the elastic cross sections were multiplied to factor $\alpha_2 q^2$ and shifted to δq, see table 1).

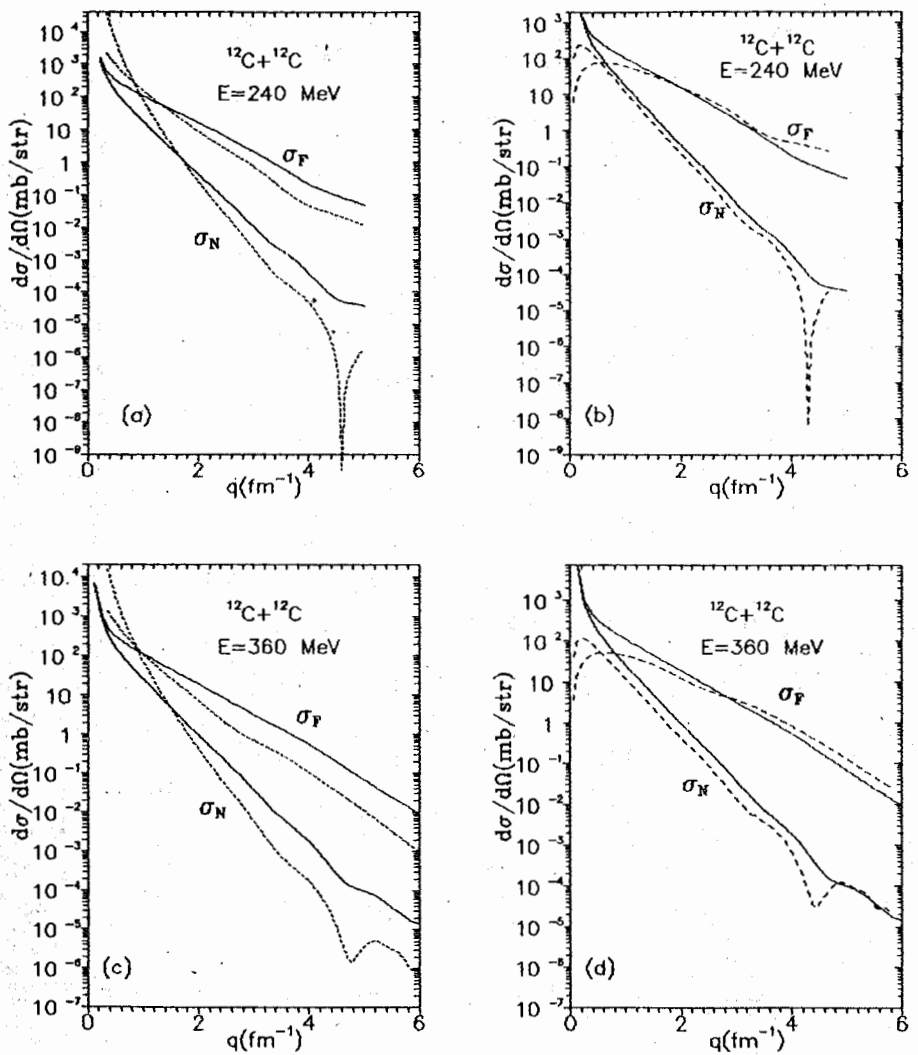

Fig.3 Decomposition of the elastic and inelastic cross sections into the near- and far-side cross sections are shown. The solid curves correspond to the inelastic scattering cross sections; the short-dashed curves in (a) and (c), to the elastic scattering cross sections multiplied by the normalization coefficient α_2; and the long-dashed ones (b) and (d), to elastic scattering cross sections shifted to δ q, multiplied by $\alpha_2 q^2$.

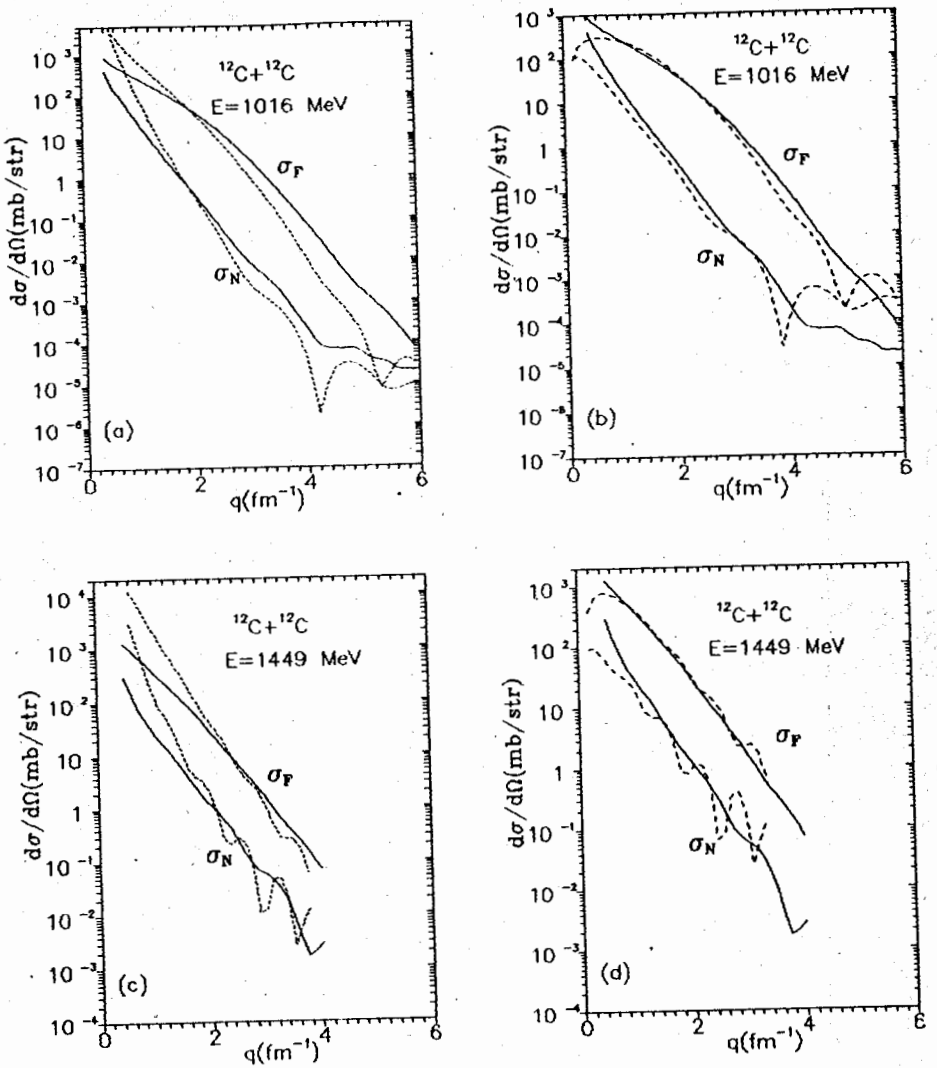

Fig.4 The same as in Fig.3, but at energies E=1016 and 1449 MeV respectively.

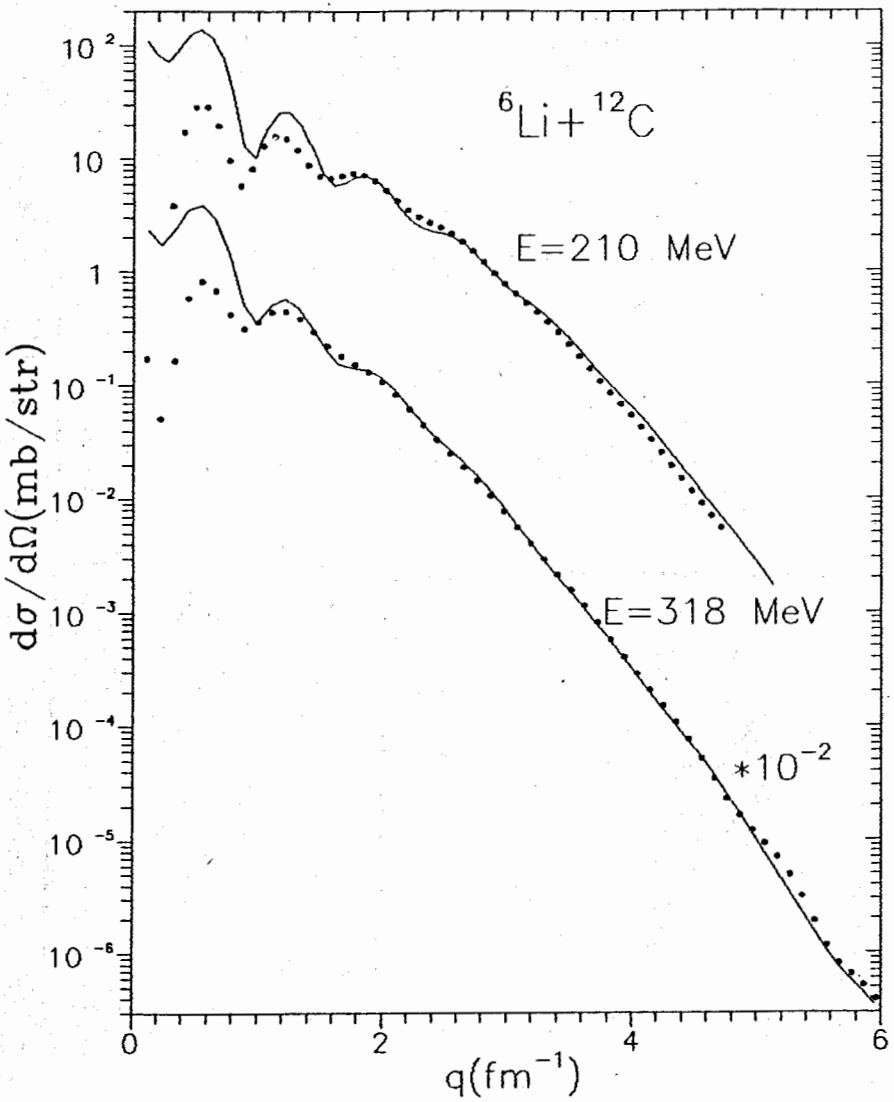

Fig.5 The same as in Fig.2, but for $^6Li +^{12} C$ by using the potentials from table 2.

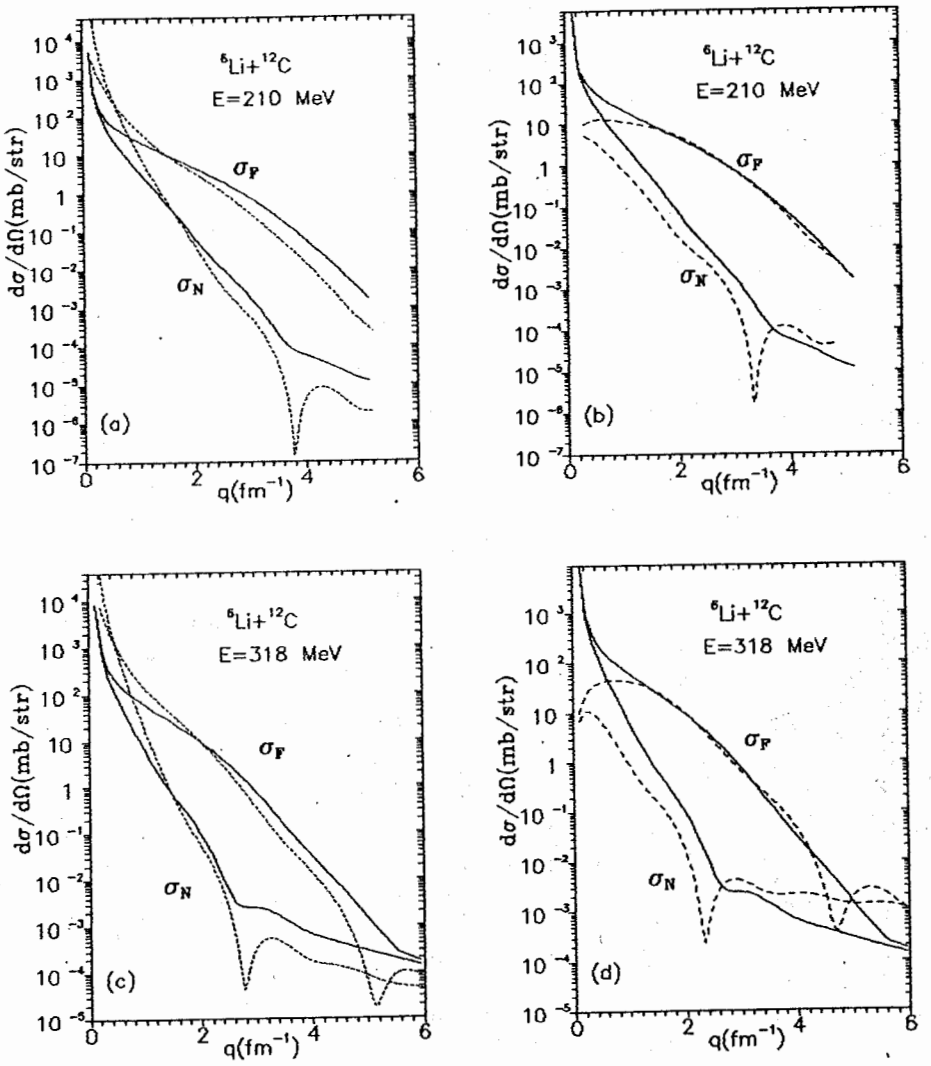

Fig.6 The same as in Fig.3, but for $^6Li +^{12} C$.

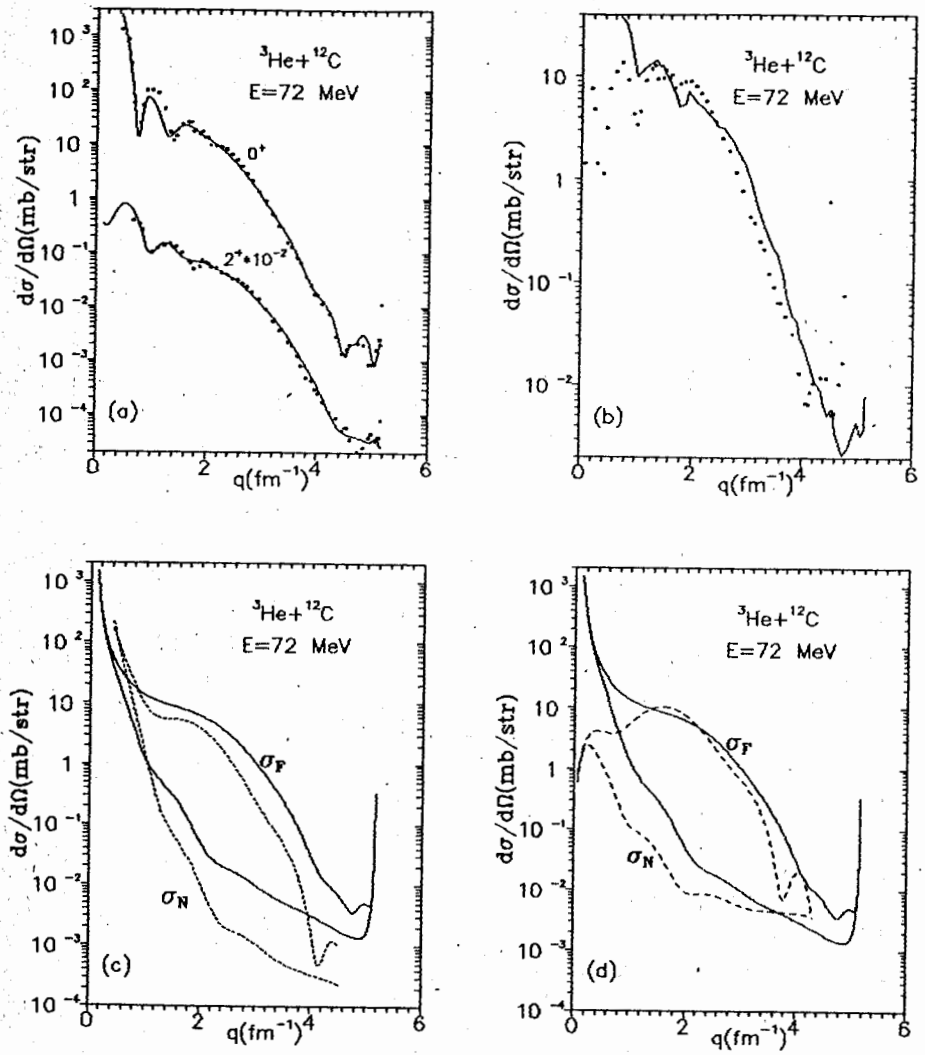

Fig.7 (a) DWBA elastic and inelastic angular distributions for the optical potentials from table 3 (solid lines) compared with data, (b), (c) and (d) the same as in Fig.2, Fig.3a and Fig.3b respectively, but for $^3He + ^{12}C$.

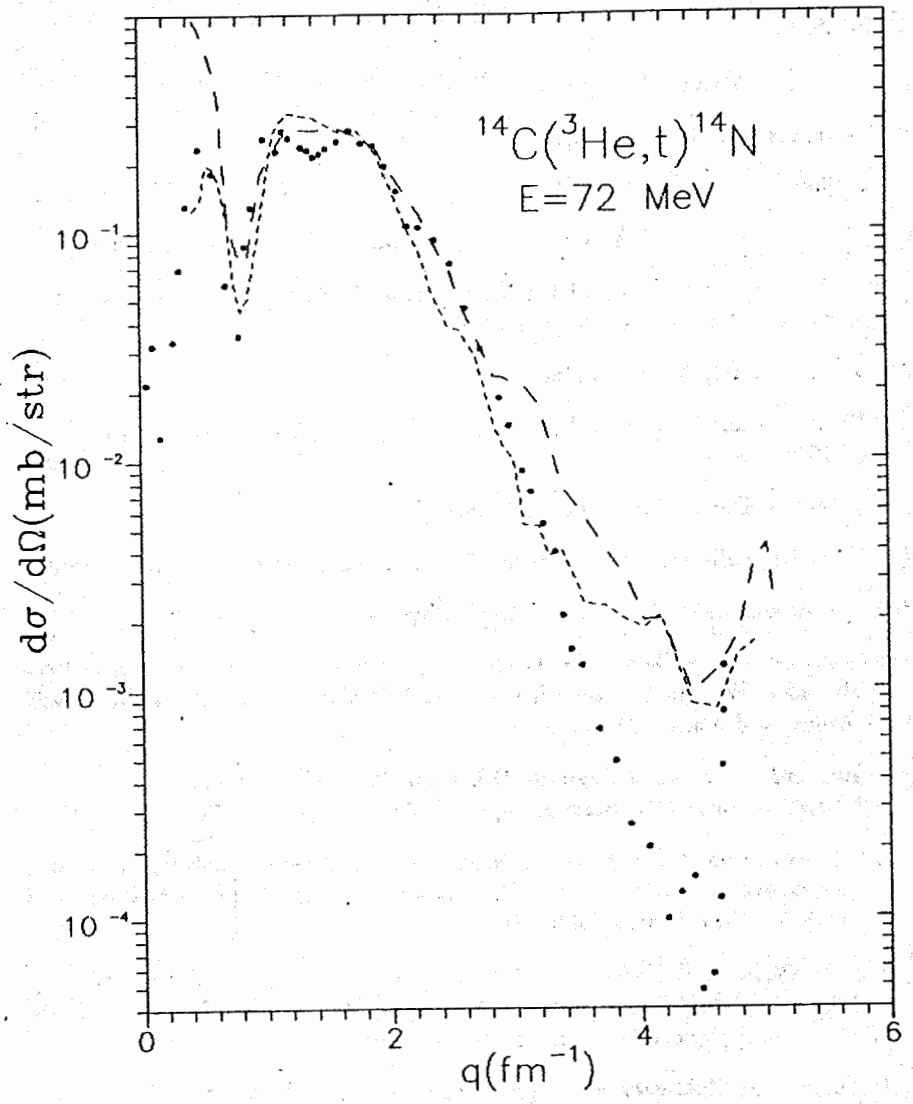

Fig.8 The correspondence between the elastic and charge-exchange cross sections. The short (long)-dashed line corresponds to the genuine $^{14}C(^3He,t)^{14}N(0^+, 2.31MeV)$ ($^{14}C(^3He,t)\ ^{14}N(1^+, 3.95MeV)$) charge-exchange scattering data with excitation of 0^+ (1^+) state; and bullets, to the calculated ones from (15) by using the elastic scattering experimental data (the elastic cross sections were multiplied by factor αq^2 and shifted to δq).

References

[1] S.I.Drosdov, ZhETF 30(1956)786.

[2] E.V.Inopin, ZhETF 31(1956)901.

[3] J.S.Blair, Phys. Rev. 115(1959)928.

[4] R.D.Amado, F.Lenz, J.A.McNeil and D.A.Sparrow, Phys. Rev. C22(1980)2094.

[5] M.S.Hussein, Invited Talk at the Notre Dame Workshop on Giant Resonances and Related Phenomena, October 21-23, 1991, Norte Dame, USA.

[6] L.J.Tassie, Aust. J. Phys. 9(1956)407.

[7] S.Hayakawa and S.Yoshida, Progr. Theor. Phys. 14(1955)1; Proc. Phys. Soc. A68(1955)656.

[8] E.V.Inopin, Doctoral dissertation (1967).

[9] W.E.Frahn, Diffractive processes in nuclear physics, Clarendon Press, Oxford.

[10] A.N.F.Aleixo and C.A.Bertulani, Nucl. Phys. A528(1991)436.

[11] H.G.Bohlen, X.S.Chen, J.G.Cramer, P.Frobrich, B.Gebauer, H.Lettau, A.Miczaika, W. von Oertzen, R.Ulrich and T.Wilpert, Zeitschrift fur Physik A- Atoms and Nuclei, 322(1985)241.

[12] M.Buenerd, A.Lounis, J.Chauvin, D.Lebrun, P.Martin, G.Dunamel, J.C.Gondrand and P.De Saintignon, Nucl. Phys. A424(1984)313.

[13] A.C.Dem'yanova, A.A.Ogloblin, S.N.Ershov, F.A.Gareev, R.S.Kurmanov, E.F.Svinareva, S.A.Goncharov, V.V.Adodin, N.Burtebaev, J.M.Bang and J.S.Vaagen, Phys. Scripta T32(1990)89.

[14] A.C.Dem'yanova, E.F.Svinareva, S.A.Goncharov, S.N.Ershov, F.A.Gareev, G.S.Kazacha, A.A.Ogloblin and J.S.Vaagen, University of Bergen Scientific/Technical Report 1991-34, Bergen, Norway.

[15] A.Nadasen, M.McMaster, M.Fingal, J.Tavormina, J.S.Winfield, R.M.Ronningen, P.Schwandt, F.D.Becchetti, J.W.Janecke and R.E.Warner, Rhys. Rev. C40(1989)1237; Phys. Rev. C39(1989)536.

[16] J.S.Winfield, B.Ashe, F.D. Becchetti, J.Brown, J.Brusoe, D.Hotz, J.Janecke, D.Roberts, P.Schwandt and G.Yoo, NSCL Annual Report 1990.

[17] A.C.Dem'yanova, A.A.Ogloblin, S.N.Ershov, F.A.Gareev, P.P.Korovin, S.A.Goncharov, Yu.A.Lyashko, A.A.Adodin and J.M.Bang, Nucl. Phys. A482(1988)383.

Received by Publishing Department
on March 16, 1992

Гареев Ф.А. и др. E4-92-113

Соотношения между сечениями упругого и неупругого рассеяния в области углов ядерной радуги

Показано, что при определенных условиях сечение неупругого рассеяния может быть выражено через сечение упругого рассеяния.

Работа выполнена в Лаборатории теоретической физики ОИЯИ.

Препринт Объединенного института ядерных исследований. Дубна 1992

Gareev F.A. et al. E4-92-113

Data-to-Data Relations Between Elastic and Inelastic Scattering in Nuclear Rainbow Region of Angles

It is shown that inelastic scattering cross sections, under suitable approximations, can be re-expressed in terms of the elastic scattering cross section.

The investigation has been performed at the Laboratory of Theoretical Physics,JINR

Preprint of the Joint Institute for Nuclear Research. Dubna 1992